Quantitative microbial ecology through stable isotope probing

Bruce A. Hungate[1,2,*], Rebecca L. Mau[1], Egbert Schwartz[1,2], J. Gregory Caporaso[1,2,3], Paul Dijkstra[1,2], Natasja van Gestel[1], Benjamin J. Koch[1], Cindy M. Liu[4,5], Theresa A. McHugh[1], Jane C. Marks[1,2], Ember Morrissey[2], Lance B. Price[4,6]

[1]Center for Ecosystem Science and Society, Northern Arizona University, Flagstaff, AZ, 86001, USA

[2]Department of Biological Sciences, Northern Arizona University, Flagstaff, AZ, 86001, USA

[3]Center for Microbial Genetics and Genomics, Northern Arizona University, Flagstaff, AZ, 86001, USA

[4]Translational Genomics Research Center, Flagstaff AZ, 86001, USA

[5]Department of Pathology, Johns Hopkins School of Medicine, Baltimore, MD 21211, USA

[6]Department of Environmental and Occupational Health, Milken Institute School of Public Health, George Washington University, Washington DC, 20037 USA

*Corresponding Author: Department of Biological Sciences, Box 5640 Northern Arizona University, Flagstaff, AZ 86011, USA; telephone: 928 699 3998, email: Bruce.Hungate@nau.edu

Abstract

Bacteria grow and transform elements at different rates, yet quantifying this variation in the environment is difficult. Determining isotope enrichment with fine taxonomic resolution after exposure to isotope tracers could help, but there are few suitable techniques. We propose a modification to Stable Isotope Probing (SIP) that enables determining the isotopic composition of DNA from individual bacterial taxa after exposure to isotope tracers. In our modification, after isopycnic centrifugation, DNA is collected in multiple density fractions, and each fraction is sequenced separately. Taxon specific density curves are produced for labeled and non-labeled treatments, from which the shift in density for each individual taxon in response to isotope labeling is calculated. Expressing each taxon's density shift relative to that taxon's density measured without isotope enrichment accounts for the influence of nucleic acid composition on density and isolates the influence of isotope tracer assimilation. The shift in density translates quantitatively to isotopic enrichment. Because this revision to SIP allows quantitative measurements of isotope enrichment, we propose to call it quantitative Stable Isotope Probing (qSIP). We demonstrate qSIP using soil incubations, in which soil bacteria exhibited strong taxonomic variation in ^{18}O and ^{13}C composition after exposure to ^{18}O-H_2O or ^{13}C-glucose. Addition of glucose increased assimilation of ^{18}O into DNA from ^{18}O-H_2O. However, the increase in ^{18}O assimilation was greater than expected based on utilization of glucose-derived carbon alone, because glucose addition indirectly stimulated bacteria to utilize other substrates for growth. This example illustrates the benefit of a quantitative approach to stable isotope probing.

Keywords: stable isotope probing, oxygen-18, ^{18}O-H_2O, biodiversity, ecosystem functioning, soil carbon cycle

Introduction

The types of organisms present in an ecosystem profoundly influence its functioning, an idea well established for plants and animals, formalized in the state factor theory of ecosystem science (1), and illustrated through the impacts of plant and animal invasions on ecosystem processes (2). The physiological and taxonomic diversity of microorganisms far exceeds that of plants and animals combined (3). Yet, despite progress applying molecular tools to analyze microbial diversity of intact assemblages (4-6), our understanding of how individual microbial taxa affect ecosystem processes like element cycling remains weak. When applied to intact microbial assemblages, stable isotope probing (SIP) partly addresses this challenge, in that it links physically the fluxes of elements to an organism's genome. In conventional SIP, organisms that utilize isotopically labeled substrates incorporate the heavy isotope into their nucleic acids, increasing the density of those nucleic acids which then migrate further along a cesium chloride density gradient formed during isopycnic centrifugation. This enables identifying organisms that utilized the labeled compound for growth (7). Conventional SIP applications use a qualitative approach that identifies visually the separation caused by isotope incorporation (7). Nucleic acids in density regions defined as "heavy" or "light" are then sequenced. Organisms disproportionately represented in the "heavy" region are interpreted as having utilized the labeled substrate for growth (8-11).

SIP is a robust technique to identify microbial populations that assimilate a labeled substrate, but it does not provide quantitative measures of assimilation rates, for three reasons. First, the distinction between labeled and unlabeled organisms is binary, defined by the density regions selected by the investigator, limiting the resolution of taxon-specific responses to labeled or unlabeled. Second, the distribution of DNA along the density gradient reflects the influences of both isotope incorporation and GC (guanine plus cytosine) content because the density of DNA increases with its GC content (12). Any comparison of density regions will reflect both influences, challenging inferences about quantitative isotope incorporation. Third, in conventional SIP there are no assurances that the identification of the labeled community is complete. Low GC content organisms that incorporated the isotope label may not have shifted sufficiently in density to be part of the "labeled" density fraction, and high GC content organisms that did not incorporate the label may be erroneously inferred to be part of the labeled community. This could result in incomplete coverage when discrete, non-contiguous, density intervals representing "heavy" and "light" fractions (13, 14) are selected for sequencing, omitting information about the microbial assemblage contained in the DNA at intermediate densities. In other cases, only the "heavy" fractions in both labeled and unlabeled treatments were sequenced and compared: any new organisms that appeared in the heavy fraction of the labeled treatment were inferred to have taken up enough of the isotope tracer to have shifted the density of their DNA (15). This approach could have excluded organisms that incorporated the isotope tracer, but did not shift sufficiently to be represented in the "heavy" fraction, because of their low GC content. In these ways, SIP as typically practiced is a qualitative technique capable of identifying

some of the organisms that utilize a substrate, not a quantitative one capable of exploring the full range of variation in isotope incorporation among microbial taxa.

Here, we describe modifications to SIP that enable quantifying isotopic incorporation into the genomes of individual taxa. We developed an approach that quantifies the baseline density of the DNA of individual taxa without exposure to isotope tracers, and then quantifies the change in DNA density of each taxon caused by isotope incorporation. Using a model of isotope substitution in DNA, we convert the observed change in density to isotope composition. We show how qSIP applies in soil incubations using a specific carbon source (^{13}C-glucose) and using a universal substrate for growing organisms (^{18}O-H_2O). We also show how combining these tracers can provide unique insight into the microbial ecology of an interesting biogeochemical phenomenon widely observed in soil for nearly a century, the priming effect (16). The "priming effect" is the phenomenon where there occurs "extra decomposition of native soil organic matter in a soil receiving an organic amendment" (17), first documented in soils over 80 years ago (18-20). This example illustrates the potential of qSIP because the priming effect involves quantitative fluxes of elements in ecosystems and some hypotheses to explain it invoke microbial biodiversity (21). This example also illustrates how techniques like qSIP could advance microbial ecology as a quantitative field, relating microbial biodiversity to element cycling at the ecosystem scale.

Methods

Soil incubations and DNA extractions

Our sample processing scheme, from soil collection, nucleic acid extraction, centrifugation, to data analysis, is summarized in Figure 1. Soil (0-15 cm) was collected in November 2012 from a ponderosa pine forest meadow, located on the C. Hart Merriam Elevation Gradient in Northern Arizona, USA (35.42N, -111.67W; http://nau.edu/ecoss/what-we-do/future-ecosystems/elevation-gradient-experiment/).. Soil was sieved (2 mm mesh), left to air-dry for 96 hours, then stored at 4°C before the experiment started. One gram of soil was added to 15 mL Falcon tubes and adjusted to 60% water holding capacity, incubated for one week, and then allowed to air dry for 48 hours prior to isotope additions. Samples were incubated for 7 days. During the incubation, samples received 200 μL of water g^{-1} soil or a glucose solution at a concentration of 500 μg C g^{-1} soil in the following isotope and substrate treatments (each with n=3): 1) water at natural abundance $\delta^{18}O$; 2) ^{18}O-enriched water (atom fraction 97%); 3) glucose and water at natural abundance $\delta^{13}C$ and $\delta^{18}O$; 4) ^{13}C-enriched glucose (atom fraction 99%) and water at natural abundance $\delta^{18}O$; 5) glucose at natural abundance $\delta^{13}C$ and ^{18}O-enriched water (atom fraction 97%). These treatments were selected in order to evaluate the effects of isotope addition on the density and isotopic composition of DNA. We assessed (I) the effect of ^{18}O in the absence of supplemental glucose as the difference between treatment 2 and 1, (II) the effect of ^{13}C in the presence of supplemental glucose as the difference between treatments 4 and 3, and (III) the effect of ^{18}O with supplemental glucose as the difference between treatments 5 and 3. In each case, these comparisons isolate the effect of the presence of an isotope tracer. The specific equations quantifying these comparisons are presented below.

After the incubation, samples were frozen and stored at -40°C. DNA was extracted from approximately 0.5 g soil using a FastDNA® Spin Kit for Soil (MP Biomedicals, Santa Ana, CA, USA) following the manufacturer's directions. Extracted DNA was quantified using the Qubit® dsDNA High-Sensitivity Assay Kit and a Qubit® 2.0 Fluorometer (Invitrogen, Eugene, OR, USA).

Density Centrifugation and Fraction Collection

To separate DNA by density, 5 μg of DNA was added to approximately 2.6 mL of a saturated CsCl and gradient buffer (200 mM Tris, 200 mM KCl, 2 mM EDTA) solution in a 3.3 mL OptiSeal™ Ultracentrifuge tube (Beckman Coulter, Fullerton, CA, USA). The final density of the solution was 1.73 g cm^{-3}. The samples were spun in an Optima™ MAX benchtop ultracentrifuge (Beckman Coulter, Fullerton, CA, USA) using a Beckman TLN-100 rotor at 127,000 x *g* for 72 hours at 18°C. After centrifugation, the density gradient was divided into fractions of 150 μL each using a fraction recovery system (Beckman Coulter Inc, Palo Alto, CA, USA). The density of each fraction was subsequently measured with a Reichert AR200 digital refractometer (Reichert Analytical Instruments, Depew, NY, USA). DNA was separated from the CsCl solution using isopropanol precipitation, resuspended in 50 μL sterile deionized water, and quantified for each density fraction. We determined total number of bacterial 16S rRNA gene copies in each density fraction by qPCR using a pan-bacterial broad-coverage quantitative PCR technique (22). All fractions were analyzed in triplicate in 10 μl reactions that included 1 μl of DNA template and 9 μl of reaction mix containing 1.8 μM of forward (5'-

CCTACGGG**D**GGC**W**GCA-3') and reverse (5'-GGACTAC**HV**GGGT**M**TCTAATC-3') primers (bold letters denote degenerate bases), 225 nM of the TaqMan® minor groove-binding probe (6FAM) 5'-CAGCAGCCGCGGTA-3' (MGBNFQ), 1x *Platinum*® Quantitative *PCR SuperMix-UDG* (Life Technologies, Grand Island, NY), and molecular-grade water. Amplification and real-time fluorescence detection were performed on the 7900HT Real Time PCR System (Applied Biosystems). We provide the qPCR data for all density fractions in the supplementary online material.

Data analysis of total 16S rRNA gene copy number

Based on the qPCR data, we produced a conventional SIP density curve by graphing the proportion of total 16S rRNA gene copies as a function of density, an approach often used to visualize the effect of isotope incorporation on the distribution of densities across the bacterial assemblage, delineating "heavy" and "light" regions for sequencing (9-11). We also calculated the average DNA density for each tube as a weighted average of the density of each fraction in which 16S rRNA gene copies were detected, weighted by the proportional abundance of total 16S rRNA gene copies measured in that fraction for each tube. This provided an estimate of the average DNA density for each tube, enabling testing via bootstrapping whether isotope addition increased the density of DNA.

Sequencing 16S rRNA genes

We sequenced the 16S rRNA gene in every density fraction that contained DNA (9-15 fractions per centrifuge tube) by a dual-indexing amplicon-based sequencing on the Illumina MiSeq

(Illumina Inc, San Diego, CA, USA) following Farosh et al, 2014 (23). For each density fraction, the 16S rRNA gene V3-V4 hypervariable region was amplified in 25 µl reactions that included 5 µl of gDNA in a 20 µl of reaction mix containing 12.5 µl Phusion High-Fidelity PCR Master Mix with HF Buffer (New England Biolabs Inc., Ipswich, MA, USA), 0.75 µl DMSO, and 1.75 µl of sterile water and 0.2 µM of each forward (5'-ACTCCTACGGGAGGCAGCAG-3') and reverse (5'-GGACTAC**HV**GGGT**W**TC-TAAT-3') primers, each concatenated to a linker sequence, a 12bp barcode, and a "heterogeneity spacer" of 0-7bp in size. The following thermocyling condition was used: an initial denaturation at 98°C for 30s, followed by 30 cycles of denaturation at 98°C for 30s, annealing at 98°C for 30s, and amplification/ extension at 72°C for 30s. The resultant amplicons were normalized and pooled using the SequelPrep Normalization Kit (Life Technologies, Carlsbad, CA, USA), then purified using the AMPure XT beads (Beckman Coulter Genomics, Danvers, MA, USA) and sequenced in combination with ~20% of PhiX control library (v3) (Illumina) on 300bp paired-end MiSeq runs.

Data-analysis

Subsequent sequence processing and quality filtering were also performed as described in Farosh et al, 2014 (23). Each read was assigned to the original sample based on the 24bp dual-index barcode formed by concatenating the 12bp barcodes from each paired-end read. After trimming the primer sequences, the original V3-V4 amplicon was reconstituted by stitching the paired-end reads without preliminary quality filtering using FLASH (24), as FLASH includes error correction. We obtained 9,378,878 high-quality stitched reads that were subsequently processed at a median length of 410 bp.

The stitched reads were clustered using the uclust-based (25) open reference OTU picking protocol (26) described in QIIME (v1.8.0-dev) (27) against the Greengenes 13_8 reference database (28). Representative sequences for each OTU were chosen as the cluster centroid sequences. OTUs with representative sequences that could not be aligned with PyNAST and OTUs with a total count of less than 2 across all samples (i.e., singleton OTUs) were excluded from subsequent analyses, leaving a total of 76,710 OTUs composed of 9,127,632 reads.

All taxonomic assignments used throughout this study were generated by QIIME's uclust-consensus taxonomy assigner (default parameters, 29) against the Greengenes 13_8 97% reference OTUs (30). The taxonomic abundances for each sample-taxa combination using the uclust-consensus assigner were compared with taxonomic assignments made with the RDP classifier (confidence = 0.5, as recommended in (31)) using a non-parametric Pearson correlation test with 999 iterations. For each sample-taxa combination, taxonomic abundances were compared for the two assignment methods (i.e., using QIIME's `compare_taxa_summaries.py` script). The resulting p-values were significant ($p<0.001$) at all taxonomic levels, and the Pearson r-values were high (>0.96, Supplemental Material Table S1), indicating that the taxonomic profiles generated by the different methods were nearly identical. Analyses here focused on taxonomic classification to the level of genus, of which the uclust consensus assignment yielded a total of 790 genera. Genera included for analysis here were the 379 that occurred in all replicate tubes; these were also the most abundant taxa, representing 99.531% of the total 16S rRNA gene copies across the dataset. All QIIME commands used in this analysis are provided in

Supplementary Information. All sequence data have been deposited at MG-RAST (32) project ID 14151.

Overview of quantitative taxon-specific isotope incorporation

In the following, we describe the calculations required to determine the isotopic composition of individual taxa after exposure to isotopically labeled substrates. In this approach, the taxon-specific density of DNA in the treatment with the isotopically labeled substrate is computed and compared to the density of DNA for the same taxon in the treatment with no added isotope tracer. For a particular element and isotope, the density of DNA will reach a maximum value when all atoms of that element in the DNA molecule are labeled with the isotope tracer. Smaller shifts in density reflect intermediate degrees of tracer incorporation; the scaling between density shift and isotope incorporation is linear after accounting for the effect of GC content on the elemental composition of DNA. The incorporation of the isotope tracer is expressed as atom fraction excess, which is the increase above natural abundance isotopic composition, and ranges from a minimum of 0 to a maximum of 1 minus the natural abundance background for a given isotope-element combination. Variables, calculated quantities, and indices are defined in Table 1.

Calculating taxon-specific weighted averaged density differences

For each fraction k of a particular replicate density gradient j, we measured the total number of 16S rRNA gene copies (f_k) using qPCR, the proportion (p_{ijk}) of total 16S rRNA gene copies for each bacterial taxon i within that fraction from sequencing, and the density (x_{jk}) of that fraction.

We calculated the total number of 16S rRNA gene copies per µL (y_{ijk}) for bacterial taxon i in density fraction k of replicate j as:

$$y_{ijk} = p_{ijk} \cdot f_{jk} \quad (1)$$

The total number of 16S rRNA gene copies (y_{ij}) for bacterial taxon i in replicate j is summed across all K density fractions:

$$y_{ij} = \sum_{k=1}^{K} y_{ijk} \quad (2)$$

The density (W_{ij}) for bacterial taxon i of replicate j was computed as a weighted average, summing across all K density fractions the density (x_{jk}) of each individual fraction times the total number of 16S rRNA gene copies (y_{ijk}) in that fraction expressed as a proportion of the total 16S rRNA gene copies (y_{ij}) for taxon i in replicate j:

$$W_{ij} = \sum_{k=1}^{K} x_{jk} \cdot \left(\frac{y_{ijk}}{y_{ij}} \right) \quad (3)$$

For a given taxon, we calculated the difference in density caused by isotope incorporation (Z_i):

$$Z_i = W_{LABi} - W_{LIGHTi} \quad (4)$$

where W_{LABi} is the mean, across all replicates, of the isotope-enriched treatment (labeled, LAB; n=3) and W_{LIGHTi} is the mean, across all replicates, of the unlabeled treatment (unlabeled, LIGHT; n=6). Because our experiment had multiple treatments without heavy isotopes, we included data from all replicate tubes in those unlabeled treatments (i.e., unlabeled treatments with and without added carbon; n=6) to estimate the unlabeled average density (W_{LIGHTi}) for each taxon i.

Calculating taxon-specific GC content and molecular weight

We calculated the GC content (G_i) of each bacterial taxon using the mean density for the unlabeled (W_{LIGHTi}) treatments (n=6). We derived the relationship between GC content and buoyant density using DNA from pure cultures of three microbial species with known but strongly differing GC content (see below). The linear relationship between GC content (G_i, expressed as a proportion) and unlabeled buoyant density (W_{LIGHTi}) on a CsCl gradient is:

$$G_i = \frac{1}{0.083506} \cdot \left(W_{LIGHTi} - 1.646057 \right) \quad (5)$$

The natural abundance molecular weight of DNA is a function of GC content, based on the atomic composition of the four DNA nucleotides. DNA made of pure adenine (A) and thymine (T) has a molecular weight of 307.691 g mol^{-1}, while DNA made up of only guanine (G) and cytosine (C) has a molecular weight of 308.187 g mol^{-1}. When GC content is known, molecular weight can be calculated using:

$$M_{LIGHTi} = 0.496 G_i + 307.691 \quad (6)$$

Percent change in molecular weight associated with isotope incorporation

The number of oxygen atoms per DNA nucleotide pair (GC and AT) is constant (6 for G and C, 7 for T, and 5 for A) regardless of GC content. These atoms contain ^{18}O at natural abundance, which we assume to be 0.002000429 atom fraction for ^{18}O and 0.0003789961 atom fraction for ^{17}O (IAEA 1995). The maximum labeling is achieved when all oxygen atoms are replaced by ^{18}O. Therefore, given the molecular weight of each additional neutron (1.008665 g mol^{-1}; 33), the maximal increase in molecular weight (corresponding to 1 atom fraction ^{18}O, or 100% atom

percent ^{18}O) is 12.07747 g mol^{-1}. Thus, the theoretical maximum molecular weight ($M_{HEAVYMAXi}$) of fully ^{18}O-labeled DNA for taxon *i* is:

$$M_{HEAVYMAXi} = 12.07747 + M_{LIGHTi} \quad (7)$$

In contrast, the number of carbon atoms per DNA nucleotide varies with GC content. There are 10 carbon atoms in G, A, and T, but only 9 in C. The average number of carbon atoms per DNA nucleotide ($H_{CARBONi}$) for taxon *i* can therefore be expressed as:

$$H_{CARBONi} = -0.5G_i + 10 \quad (8)$$

We assume these atoms are ^{13}C-labeled at natural abundance (0.01111233 atom fraction ^{13}C; 33). The maximal labeling is achieved when all carbon atoms are replaced by ^{13}C. Complete replacement of carbon atoms with ^{13}C increases the molecular weight by 9.974564 g mol^{-1} for G, A, and T, and by 8.977107 g mol^{-1} for C. Using equation 8, the theoretical maximum molecular weight ($M_{HEAVYMAXi}$) of fully ^{13}C-labeled DNA can be calculated as follows, with GC content (G_i) expressed as a fraction:

$$M_{HEAVYMAXi} = -0.4987282Gi + 9.974564 + M_{LIGHTi} \quad (9)$$

Calculating isotope enrichment from density shifts

We calculated the proportional increase in density (Z_i) relative to the density of the unlabeled treatments (W_{LIGHTi}), and calculated molecular weight of DNA for taxon *i* in the labeled treatment (M_{LABi}) as:

$$M_{LABi} = \left(\frac{Z_i}{W_{LIGHTi}} + 1 \right) \cdot M_{LIGHTi} \quad (10)$$

The atom fraction excess of ^{18}O for taxon *i* ($A_{OXYGENi}$) is then calculated as:

$$A_{OXYGENi} = \frac{M_{LABi} - M_{LIGHTi}}{M_{HEAVYMAXi} - M_{LIGHTi}} \cdot (1 - 0.002000429) \quad (11)$$

We used the results from a pure culture study with *E. coli*, grown with variable ^{18}O-enriched water (natural abundance, 5, 25, 50, and 70% atom fraction ^{18}O; see below) to compare to the theoretical calculations of atom fraction excess ^{18}O derived above.

Similarly, the atom fraction excess ^{13}C for taxon *i* ($A_{CARBONi}$) was calculated as:

$$A_{CARBONi} = \frac{M_{LABi} - M_{LIGHTi}}{M_{HEAVYMAXi} - M_{LIGHTi}} \cdot (1 - 0.01111233) \quad (12)$$

Pure culture studies

To verify the predicted relationship between increased density and atom fraction excess we conducted experiments with a pure *Escherichia coli* culture. *E. coli* (strain HB101, GC content 50.8%) was shaken at 100 rpm, 37 °C for 8 h in Luria-Bertani (LB) broth that was prepared with a mixture of natural abundance and ^{18}O-water to achieve five ^{18}O-enrichment levels (natural abundance, 5, 25, 50, and 70% atom fraction ^{18}O). Genomic DNA was extracted in triplicate using PowerLyzer UltraClean Microbial DNA Isolation Kit according to the manufacturer's instructions (MO BIO Laboratories, Inc., Carlsbad, CA). We also grew pure cultures of two additional strains of bacteria selected for low GC content (*Staphylococcus epidermidis*, ATTC# 49461, 32.1%) and high GC content (*Micrococcus leuteus*, ATTC# 49732, 73%). *S. epidermidis* was grown for 24 h on Brain Heart Infusion Agar at 37 °C, and *M. leuteus* was grown with LB agar at 23 °C. These cultures were grown with substrates and water at natural abundance stable isotope composition.

For each culture, genomic DNA was extracted in triplicate. Approximately 800 ng of each DNA extract was used for isopycnic centrifugation, density quantification, and DNA isotope analysis. The ^{18}O composition of the *E. coli* DNA was determined with a PyroCube (Elementar Analysensysteme GmbH, Hanau, Germany) interfaced to a PDZ Europa 20-20 isotope ratio mass spectrometer (Sercon Ltd., Cheshire, UK) at the UC Davis Stable Isotope Facility (Davis, CA). Samples were prepared by diluting the *E. coli* DNA with natural abundance salmon sperm DNA to achieve enrichment levels below 100 ‰ $\delta^{18}O$ for isotope analysis. Densities of DNA from the cultures grown at natural abundance isotope composition were used to determine the relationship between the density of DNA and its GC content, yielding the relationship described in Eq. 5 (r^2 = 0.912, $P < 0.001$).

Statistical analysis

Following the equations above, we computed the difference in densities, Z_i, between treatments with and without isotope tracers, and the corresponding values of isotope composition, A_{OXYGEN} and A_{CARBON}. We used bootstrap resampling (with replacement, 1000 iterations) of replicates within each treatment to estimate taxon-specific 90% confidence intervals for the change in density and the corresponding value of atom fraction excess isotope composition. All calculations were performed in R (R Core Team 2014).

Density fractionation separates organisms according to GC content (12) as well as isotope incorporation, so traditional SIP may be biased toward identifying high-GC content organisms as growing or utilizing a substrate (34, 35). To test whether qSIP exhibited any such bias, we used density without isotope addition as a proxy for GC content, and tested whether the densities of

organisms identified as assimilating (90% confidence intervals did not include 0 for A_{CARBON} or A_{OXYGEN}) differed in density from organisms where assimilation was not detected.

Our focus was on the magnitude of variation in Z_i, A_{OXYGEN}, and A_{CARBON}, because the goal of our work is to establish a means to discern from SIP experiments quantitative estimates of isotope tracer uptake. These values lie along a continuum from no uptake to complete isotope replacement, and our approach provides a means to estimate the values and place confidence limits on those estimates (rather than, for example, placing a high priority on distinguishing values that are significantly positive from those that are not). For this reason, we selected bootstrap resampling rather than, for example, t-tests. We note that, in typical SIP experiments, an organism is considered to be growing or utilizing a substrate if it exhibits a change in relative abundance when comparing the heavy fraction of the labeled versus control (e.g., 10) or comparing the heavy fraction versus the light fraction (e.g., 36), yet assessments of variation in these estimates are not typically presented. Our approach assesses both the quantitative values of isotope uptake and the variation associated with those estimates.

Results

In the pure culture experiments, the ^{18}O composition of *E. coli* DNA was strongly related to the ^{18}O composition of water in the growth medium, supporting the notion that oxygen from water is quantitatively incorporated into the DNA of growing organisms ($P<0.001$, $r^2 = 0.976$, Figure 2A). The slope of the relationship, 0.334 ± 0.017 (n=15), indicates that 33% of oxygen in *E. coli* DNA was derived from water. The shift in density of *E. coli* DNA with ^{18}O incorporation matched well the theoretical prediction of the model of isotope substitution in the DNA molecule (Equations 10 and 11, Figure 2B). These results confirm that ultracentrifugation in CsCl can serve as a quantitative mass separation procedure, resolving variation in isotope tracer incorporation into DNA. These results also support our model of the relationship between the density of nucleic acids and isotopic substitution in the DNA molecule.

In soil incubations, DNA density averaged across the entire community tended to increase in response to isotope addition (Figure 3). Addition of ^{13}C-glucose (Figure 3A) increased the density of DNA by 0.0043 g cm^{-3}, but the 90% confidence interval for this increase overlapped zero (-0.002 to 0.0091 g cm^{-3}). Addition of ^{18}O-water (Figure 3B) caused a similar increase in density, 0.0041 g cm^{-3}, but the 90% confidence interval for this increase also overlapped zero, spanning -0.0011 to 0.0090 g cm^{-3}. The incubations receiving ^{18}O-water and supplemental glucose (natural abundance isotope composition) exhibited the largest increase in average DNA density, 0.0090 g cm^{-3}, and in this case the 90% confidence limit did not overlap zero (0.0065 to 0.0125 g cm^{-3}). These comparisons estimate the change in density of DNA fragments encoding the 16S rRNA gene across all taxa considered together. Figure 3 also illustrates the density

distributions often used in SIP experiments to visualize the qualitative cutoff between labeled and unlabeled regions suitable for sequencing.

Sequencing all fractions allowed visualizing analogous density distributions for individual taxa. Figure 4 shows three taxa to illustrate the concept, showing graphically the manner in which the density of labeled (W_{LABi}) and unlabeled (W_{LIGHTi}) DNA is calculated for each taxon (equation 3). For example, the density of an unidentified genus in the family Micrococcaceae did not change with ^{18}O-water addition in the absence of supplemental glucose. For this taxon, the shift in density (Z) due to ^{18}O incorporation was -0.0002 g cm^{-3}, with the 90% confidence interval spanning -0.0046 to 0.0049 g cm^{-3} (Figure 4A). The shift in density due to ^{18}O-incorporation increased when unlabeled glucose was also added (Figure 4B, Z = 0.0169 g cm^{-3}, 90% CI, 0.0146 to 0.0194 g cm^{-3}). This bacterial taxon was therefore not incorporating the ^{18}O tracer in unamended soil, but synthesized new DNA using ^{18}O derived from H_2O in response to glucose addition. The DNA of an unidentified genus in the family Pseudonocardiaceae similarly exhibited no change in density in the absence of supplemental glucose (Z = 0.0005 g cm^{-3}, -0.0033 to 0.0045 g cm^{-3}), and exhibited only a slight increase in response to glucose addition (Z = 0.0040 g cm^{-3}, 0.0015 to 0.0070 g cm^{-3}, Figure 4C & D). By contrast, the density of DNA in a member of the genus *Herpetosiphonales* increased in soil without any supplemental glucose (Z = 0.0124 g cm^{-3}, 90% CI, 0.0105 to 0.0143 g cm^{-3}, Figure 4E), but the density did not further increase in response to the addition of glucose (Z = 0.0110 g cm^{-3}, 90% CI, 0.0088 to 0.0133 g cm^{-3}, Figure 4F). These results show that, by dividing the density gradient into multiple fractions

and sequencing each separately, one can determine changes in the density of DNA for individual taxa caused by the assimilation of stable isotope tracers.

The taxon-specific shifts in average density associated with incorporation of the heavy isotope (Figure 5) translate directly to quantitative variation in isotope composition, expressed here as atom fraction excess ^{18}O (A_{OXYGEN}, Figure 5A & B) and ^{13}C (A_{CARBON}, Figure 5C). The detection limit for a shift in density is the median change in density required to shift the lower bound of the bootstrapped 90% confidence limit above zero. As constrained by our sampling design, these values were 0.0037 g cm^{-3} for ^{18}O, and 0.0044 g cm^{-3} for ^{13}C, changes that correspond to 0.056 atom fraction excess ^{18}O and 0.081 atom fraction excess ^{13}C.

More than half of the bacterial genera (209) did not exhibit any detectable excess ^{18}O enrichment under control conditions without added glucose (Figure 5A). Of the 170 taxa that did exhibit detectable ^{18}O enrichment without added glucose, the corresponding values of atom fraction excess ^{18}O ranged from 0.047 (90% confidence interval, 0.001 to 0.100) in a member of the genus, Lentzea, to 0.354 (CI, 0.248 to 0.449) in an unidentified representative of the candidate bacterial phylum, OD1. With added glucose, 351 of the 379 taxa exhibited positive atom fraction excess ^{18}O (90% CIs did not overlap zero), averaging 0.147 atom fraction excess ^{18}O (Figure 5B), with a minimum of 0.036 (CI, 0.004 to 0.064) in an unidentified genus of the family Ktedonobacteracea, and a maximum of 0.365 (CI, 0.282 to 0.449) in an unidentified genus within the class AT12OctB3 of the phylum, Bacteroidetes. Bacterial taxa in this soil varied in atom fraction excess ^{18}O under control conditions and in response to added glucose (Figure 5A

& B). Atom fraction excess ^{13}C reflects direct assimilation of C from the added glucose (Figure 5C), and ranged from no detectable enrichment among 215 of the 379 genera, to over half of the carbon atoms comprising ^{13}C in the DNA of a member of the Micrococcaceae (0.525, CI 0.458 to 0.592).

GC Bias

There was no evidence of GC bias in qSIP. Average densities of organisms exhibiting tracer assimilation were negligible for all comparisons (Table 2). Inferred GC contents averaged 52.3% (CI 44.6% to 57.3%) for organisms exhibiting tracer assimilation, very close to the average of 52.8% inferred GC content for taxa for which assimilation was not detected (CI 45.1% to 58.2%).

Soil Incubations: multi-element quantitative stable isotope probing

There was a strong positive relationship between increased atom fraction excess ^{18}O in response to glucose addition and the direct utilization of glucose-derived carbon (atom fraction excess ^{13}C) (Figure 6; r^2=0.51, P<0.001). The expected relationship (solid line in Figure 6) reflects the case where glucose is the sole C source, and thus there should be an 0.33 atom fraction excess increase in ^{18}O for each 1 atom fraction excess increase in ^{13}C, based on our finding that 33% of the oxygen molecules in DNA are derived from water (Figure 2). For many taxa, the increase in atom fraction excess ^{18}O in response to added glucose exceeded the expected amount (solid line in Figure 6).

Discussion

We demonstrate that stable isotope probing of bacterial assemblages in natural environments can yield quantitative information about the assimilation of isotope tracers into bacterial DNA with fine taxonomic resolution. This work establishes a framework for coupling quantitative interpretation of stable isotope tracer experiments with microbial diversity, a coupling essential for understanding how to represent microbial diversity in biogeochemical models.

The shifts in density we could detect using qSIP (0.0034 to 0.0042 g cm^{-3}, Figure 5) are nearly an order of magnitude smaller than those typically used to resolve the assimilation of stable isotopes into newly synthesized DNA using conventional SIP, in which "light" and "heavy" density fractions often differ by 0.03 g cm^{-3} (14, 37) or more (13, 38, 39). For ^{13}C, the minimum required change in density for SIP has been estimated to be 0.01 g cm^{-3}, corresponding to 0.2 atom fraction excess (7). The approach presented here achieves higher resolution by accounting for taxonomic differences in the density of DNA caused by natural variation in GC content. It may be possible to improve the resolution we achieved. We collected fractions in discrete density increments of 0.0036 g cm^{-3} (average difference in density between adjacent fractions), setting a limit on the changes in density we could detect. This difference in density between adjacent fractions we collected is comparable to the density shifts of bacterial taxa that we could resolve: the mean density shift required for the lower confidence limit to exceed zero was, on average, 0.0034 g cm^{-3} for ^{18}O and 0.0042 g cm^{-3} for ^{13}C. Thus, it is possible that separation of

464 the nucleic acids into finer density fractions will afford higher precision in the estimates of stable
465 isotope composition.
466 The resolution achieved by sequencing individual density fractions, though an improvement over
467 traditional SIP, is still very coarse compared to the resolution achieved with isotope ratio mass
468 spectrometry. Detecting differences between taxa with quantitative stable isotope probing (~0.05
469 atom fraction excess) is four orders of magnitude less precise than that achieved with gas isotope
470 ratio analysis of bulk organic matter in continuous flow, where differences of 0.000005 atom
471 fraction excess or better (<0.5‰) can be resolved (40). Isopycnic centrifugation to quantify
472 isotope composition is also less precise than compound specific analysis of biomarkers, for
473 example, of ^{13}C in fatty acids, where resolution of 0.00002 atom fraction excess (or 2‰) is
474 typical (41-43). Coupling stable isotope tracing with Nano-scale secondary ion mass
475 spectrometry (Nano-SIMS) and microarrays, a coupling called Chip-SIP (44), can resolve 0.005
476 atom fraction excess for ^{15}N and 0.001 for ^{13}C (45), considerably more precise than qSIP.
477
478 qSIP has advantages in taxonomic resolution over these other techniques. For compound specific
479 biomarkers, specific fatty acids serve as biomarkers for up to a dozen groups of microorganisms,
480 taxonomic resolution much coarser than that afforded by qSIP. Chip-SIP requires nucleic acid
481 probes, necessitating deciding *a priori* what sequences to collect for isotopic analysis, and
482 preparing microarrays implanted with those sequences prior to the isotope addition. For this
483 reason, in Chip-SIP the taxonomic resolution in the isotope fluxes is influenced by information
484 gathered without knowledge of which taxa are biogeochemically important. One advantage of
485 qSIP is that sequencing occurs after isotope enrichment, enabling quantitative exploration of the

biodiversity involved in biogeochemistry, without having to decide where to focus *a priori*. Furthermore, the taxonomic resolution possible with a microarray is limited by probe specificity and fidelity, whereas the resolution afforded by qSIP is very high, equivalent to the resolution of sequencing technology applied to the density fractions. Chip-SIP also requires access to a Nano-SIMS, expensive and technically challenging, limiting its wide adoption in the field.

Other approaches used to link element fluxes to microbial taxa are limited to target organisms, such as fluorescent *in situ* hybridization (FISH) coupled with SIMS (46), or halogen in situ-hybridization-SIMS (47). Bromodeoxyuridine (BrdU) uptake has been proposed as a universal technique for identifying growing organisms (48) and their responses to environmental perturbations (49). However, there is up to 10-fold variation among taxa in the conversion between BrdU uptake and growth, unrelated to taxonomic affiliation, a bias calling into question the quantitative universality of this technique (50). Compared to these other techniques, qSIP can assess quantitatively the entire microbial assemblage at fine taxonomic resolution, a solid foundation for exploring quantitatively the relationships between microbial biodiversity and the biogeochemistry known to be microbial.

Our finding that many bacterial taxa did not exhibit any increase in ^{18}O content under control conditions (Figure 5A) is consistent with the notion that a portion of the soil microbial biomass is not growing and may be metabolically inactive (51). The increase in atom fraction ^{18}O and ^{13}C with added glucose indicates that glucose addition stimulates bacterial growth, not just respiration. The breadth of taxa that exhibited a positive response to glucose addition is

consistent with glucose being a widely utilized substrate (52), though there are two other possible mechanisms. First, over the 7-day duration of the incubation period, glucose will be assimilated by cells that then died, releasing labeled cellular constituents available to the rest of the microbial community (53). We cannot distinguish between direct utilization of the added glucose and utilization of labeled cellular constituents produced by another organism. This applies equally to the ^{18}O-labeled and ^{13}C-labeled assemblages. Second, ^{18}O-water is a universal tracer for DNA synthesis, not necessarily tied to any particular carbon source (54, 55). The observed increase in atom fraction excess ^{18}O includes growth stimulation caused by the carbon contained in the added glucose, along with the growth stimulation caused by increased rates of utilization of other carbon sources. In contrast, atom fraction excess ^{13}C in response to ^{13}C-glucose addition traces the incorporation of carbon atoms from glucose (or derived from glucose via other metabolites as discussed above) into newly synthesized DNA (Figure 5C). This is expected, because glucose addition stimulates growth and DNA synthesis (56, 57). In summary, the effect of added glucose was apparent as: (1) an overall stimulation of growth, independent of the specific carbon substrate, and (2) as a stimulation of growth that relied directly on glucose-derived carbon.

The combination of ^{18}O and ^{13}C tracers enabled quantitative partitioning of these direct and indirect effects, based on the deviation in the data from the expected relationship between ^{18}O and ^{13}C enrichment for organisms utilizing glucose as a sole carbon source (solid line, Figure 6). One explanation for this deviation is that most taxa derive more than 33% of the oxygen in DNA from environmental water. Quantitative variation in the contribution of water to oxygen in DNA

could occur, for example, due to the variation in the oxidation state of the carbon substrate (e.g., lipids versus carbohydrates), though to our knowledge this variation is not known. Given the universality of the mechanism of DNA replication, it is unlikely that taxa vary widely in the contribution of water to oxygen, at least when grown on a common substrate.

A more parsimonious explanation of the deviation we observed is that it represents utilization of C sources other than glucose for growth. In other words, the added glucose stimulated the utilization of native soil C as a growth substrate. This points to the potential for quantitative stable isotope probing to test hypotheses regarding microbial diversity in the commonly observed phenomenon where the addition of simple C substrates to soil increases the mineralization of native soil C (16). This so-called "priming effect" has been observed for decades (17, 18), is common and quantitatively significant (16), but remains mechanistically inscrutable. Our results suggest that some microorganisms respond to glucose addition by enhancing their rates of utilization of native soil carbon, enabling additional biosynthesis (Figure 6). The taxonomic diversity of responses we observed highlights the potential for this technique to provide insight into the population and community ecology behind biogeochemical phenomena involving such indirect effects (e.g., 16, 17).

Quantifying isotope composition is the first step in determining the rate of substrate utilization in isotope tracer experiments, and the foundation for comparing rates of substrate utilization and element fluxes among different taxa in intact microbial communities. This work advances a quantitative approach to stable isotope probing in order to elucidate taxon-specific processes that

drive element cycling in intact communities, bringing to microbial ecology the power of stable isotopes to quantify rates of element fluxes into and through organisms (58, 59). Like Chip-SIP (44, 60), qSIP provides a means to quantify the ecology of organisms about which we know little more than the genetic fragment used to identify their unique place on the tree of life. These approaches lay the groundwork for a quantitative understanding of microbial ecosystems, including the types of ecological interactions previously described among macro-organisms that influence ecosystem processes. Quantitative stable isotope probing adds to the suite of tools that facilitate interpretation of stable isotope tracer experiments in microbial communities, probing the quantitative significance of microbial taxa for biogeochemical cycles in nature.

Acknowledgements. This research was supported by grants from the National Science Foundation (EAR-1124078 and DEB-1321792) and the Department of Energy's Biological Systems Science Division, Program in Genomic Science.

References

1. **Jenny H.** 1941. Factors of Soil Formation: A System of Quantitative Pedology. Dover Publications, New York.

2. **Vitousek PM.** 1990. Biological Invasions and Ecosystem Processes - Towards an Integration of Population and Ecosystem Studies. Oikos **57:**7-13.

3. **Pace NR.** 1997. A molecular view of microbial diversity and the biosphere. Science **276:**734-740.

4. **Amann RI, Ludwig W, Schleifer KH.** 1995. Phylogenetic Identification and in situ Detection of Individual Microbial Cells without Cultivation. Microbiological Reviews **59:**143-169.

5. **Muyzer G, Dewaal EC, Uitterlinden AG.** 1993. Profiling of Complex microbial-Populations by Denaturing Gradient Gel-Electrophoresis Analysis of Polymerase Chain Reaction-Amplified Genes Coding for 16S Ribosomal-RNA. Applied and Environmental Microbiology **59:**695-700.

6. **Roesch LF, Fulthorpe RR, Riva A, Casella G, Hadwin AKM, Kent AD, Daroub SH, Camargo FAO, Farmerie WG, Triplett EW.** 2007. Pyrosequencing enumerates and contrasts soil microbial diversity. Isme Journal **1:**283-290.

7. **Radajewski S, Ineson P, Parekh NR, Murrell JC.** 2000. Stable-isotope probing as a tool in microbial ecology. Nature **403:**646-649.

8. **Hutchens E, Radajewski S, Dumont MG, McDonald IR, Murrell JC.** 2004. Analysis of methanotrophic bacteria in Movile Cave by stable isotope probing. Environmental Microbiology **6:**111-120.

9. **Sharp CE, Martinez-Lorenzo A, Brady AL, Grasby SE, Dunfield PF.** 2014. Methanotrophic bacteria in warm geothermal spring sediments identified using stable-isotope probing. FEMS microbiology ecology **90**.

10. **Schwartz E, Van Horn DJ, Buelow HN, Okie JG, Gooseff MN, Barrett JE, Takacs-Vesbach CD.** 2014. Characterization of growing bacterial populations in McMurdo Dry Valley soils through stable isotope probing with O-18-water. Fems Microbiology Ecology **89:**415-425.

11. **Mau RL, Liu CM, Aziz M, Schwartz E, Dijkstra P, Marks JC, Price LB, Keim P, Hungate BA.** 2014. Linking soil bacterial diversity and soil carbon stability. The ISME Journal **in press**.

12. **Schildkraut CL.** 1962. Determinatino of Base Composition of Deoxyribonucleic Acid from its Buoyant Denstiy in CsCl. Journal of Molecular Biology **4:**430-&.

13. **Schmidt O, Horn MA, Kolb S, Drake HL.** 2015. Temperature impacts differentially on the methanogenic food web of cellulose-supplemented peatland soil. Environmental microbiology **17**.

14. **Aanderud ZT, Jones SE, Fierer N, Lennon JT.** 2015. Resuscitation of the rare boisphere contributes to pulses of ecosystem activity. Frontiers in Microbiology **6**.

15. **Jayamani I, Cupples AM.** 2015. Stable Isotope Probing and High-Throughput Sequencing Implicate Xanthomonadaceae and Rhodocyclaceae in Ethylbenzene Degradation. Environmental Engineering Science **32:**240-249.

16. **Kuzyakov Y, Friedel JK, Stahr K.** 2000. Review of mechanisms and quantification of priming effects. Soil Biology & Biochemistry **32:**1485-1498.

17. **Bingeman CW, Varner JE, Martin WP.** 1953. The effect of the addition of organic materials on the decomposition of an organic soil. Soil Science Society of America Proceedings **17:**34-38.

18. **Lohnis.** 1926. Nitrogen availability of green manures. Soil Science Society of America Journal **22:**171-177.

19. **Broadbent FE.** 1948. Nitrogen release and carbon loss from soil organic matter during decomposition of added plant residues. Proceedings Soil Science Society of America, 1947 **12:**246-249.

20. **Broadbent FE, Bartholomew WV.** 1949. The effect of quantity of plant material added to soil on its rate of decomposition. Proceedings Soil Science Society of America, 1948 **13:**271-274.

21. **Blagodatskaya E, Kuzyakov Y.** 2008. Mechanisms of real and apparent priming effects and their dependence on soil microbial biomass and community structure: critical review. Biology and Fertility of Soils **45:**115-131.

22. **Liu CM, Aziz M, Kachur S, Hsueh P-R, Huang Y-T, Keim P, Price LB.** 2012. BactQuant: An enhanced broad-coverage bacterial quantitative real-time PCR assay. Bmc Microbiology **12**.

23. **Fadrosh DW, Ma B, Gajer P, Sengamalay N, Ott S, Brotman RM, Ravel J.** 2014. An improved dual-indexing approach for multiplexed 16S rRNA gene sequencing on the Illumina MiSeq platform. Microbiome **2:**6-6.

24. **Magoc T, Salzberg SL.** 2011. FLASH: fast length adjustment of short reads to improve genome assemblies. Bioinformatics **27:**2957-2963.

25. **Edgar RC.** 2010. Search and clustering orders of magnitude faster than BLAST. Bioinformatics **26:**2460-2461.

26. **Rideout JR, He Y, Navas-Molina JA, Walters WA, Ursell LK, Gibbons SM, Chase J, McDonald D, Gonzalez A, Robbins-Pianka A, Clemente JC, Gilbert JA, Huse SM, Zhou HW, Knight R, Caporaso JG.** 2014. Subsampled open-reference clustering creates consistent, comprehensive OTU definitions and scales to billions of sequences. PeerJ **2:**e545.

27. **Caporaso JG, Kuczynski J, Stombaugh J, Bittinger K, Bushman FD, Costello EK, Fierer N, Pena AG, Goodrich JK, Gordon JI, Huttley GA, Kelley ST, Knights D, Koenig JE, Ley RE, Lozupone CA, McDonald D, Muegge BD, Pirrung M, Reeder J, Sevinsky JR, Turnbaugh PJ, Walters WA, Widmann J, Yatsunenko T, Zaneveld J, Knight R.** 2010. QIIME allows analysis of high-throughput community sequencing data. Nat Methods **7:**335-336.

28. **McDonald D, Price MN, Goodrich J, Nawrocki EP, DeSantis TZ, Probst A, Andersen GL, Knight R, Hugenholtz P.** 2012. An improved Greengenes taxonomy with explicit ranks for ecological and evolutionary analyses of bacteria and archaea. ISME J **6:**610-618.

29. **Bokulich NA, Rideout JR, Kopylova E, Bolyen E, Patnode J, Ellett Z, McDonald D, Wolfe B, Maurice CF, Dutton RJ, Turnbaugh PJ, Knight R, Caporaso JG.** 2015. A standardized, extensible framework for optimizing classification improves marker-gene taxonomic assignments. PeerJ PrePrints.

30. **McDonald D, Price MN, Goodrich J, Nawrocki EP, DeSantis TZ, Probst A, Andersen GL, Knight R, Hugenholtz P.** 2012. An improved Greengenes taxonomy with explicit ranks for ecological and evolutionary analyses of bacteria and archaea. ISME J **6:**610-618.

31. **Claesson MJ, O'Sullivan O, Wang Q, Nikkila J, Marchesi JR, Smidt H, de Vos WM, Ross RP, O'Toole PW.** 2009. Comparative analysis of pyrosequencing and a phylogenetic microarray for exploring microbial community structures in the human distal intestine. PLoS One **4:**e6669.

32. **Meyer F, Paarmann D, D'Souza M, Olson R, Glass EM, Kubal M, Paczian T, Rodriguez A, Stevens R, Wilke A, Wilkening J, Edwards RA.** 2008. The metagenomics RAST server - a public resource for the automatic phylogenetic and functional analysis of metagenomes. BMC Bioinformatics **9:**386.

33. **Mojr PJ, Taylor BN, Newell DB**. 2015. The 2014 CODATA Recommended Values of the Fundamental Physical Constants" (Web Version 7.0). This database was developed by J. Baker, M. Douma, and S. Kotochigova. Available: http://physics.nist.gov/constants [2-Jul-2015 16:26:15 EDT]. National Institute of Standards and Technology, Gaithersburg, MD 20899.

34. **Rangel-Castro JI, Killham K, Ostle N, Nicol GW, Anderson IC, Scrimgeour CM, Ineson P, Meharg A, Prosser JI.** 2005. Stable isotope probing analysis of the influence of liming on root exudate utilization by soil microorganisms. Environmental Microbiology **7:**828-838.

35. **Kovatcheva-Datchary P, Egert M, Maathuis A, Rajilic-Stojanovic M, de Graaf AA, Smidt H, de Vos WM, Venema K.** 2009. Linking phylogenetic identities of bacteria to starch fermentation in an in vitro model of the large intestine by RNA-based stable isotope probing. Environmental Microbiology **11:**914-926.

36. **Darjany LE, Whitcraft CR, Dillon JG.** 2014. Lignocellulose-responsive bacteria in a southern California salt marsh identified by stable isotope probing. Frontiers in Microbiology **5**.

37. **Hu HW, Macdonald CA, Trivedi P, Holmes B, Bodrossy L, He JZ, Singh BK.** 2015. Water addition regulates the metabolic activity of ammonia oxidizers responding to environmental perturbations in dry subhumid ecosystems. Environmental Microbiology **17:**444-461.

38. **Neufeld JD, Vohra J, Dumont MG, Lueders T, Manefield M, Friedrich MW, Murrell JC.** 2007. DNA stable-isotope probing. Nature Protocols **2:**860-866.

39. **Jiang XJ, Hou XY, Zhou X, Xin XP, Wright A, Ji ZJ.** 2015. pH regulates key players of nitrification in paddy soils. Soil Biology & Biochemistry **81:**9-16.

40. **Brenna JT, Corso TN, Tobias HJ, Caimi RJ.** 1997. High-precision continuous-flow isotope ratio mass spectrometry. Mass Spectrometry Reviews **16:**227-258.

41. **Amelung W, Brodowski S, Sandhage-Hofmann A, Bol R.** 2008. Combining biomarkder with stable isotope analyses for assessing the transformation and turnover of soil organic matter, p 155-250. *In* Sparks DL (ed), Advances in Agronomy, Vol 100, vol 100.

42. **Kramer C, Gleixner G.** 2008. Soil organic matter in soil depth profiles: Distinct carbon preferences of microbial groups during carbon transformation. Soil Biology & Biochemistry **40:**425-433.

43. **Treonis AM, Ostle NJ, Stott AW, Primrose R, Grayston SJ, Ineson P.** 2004. Identification of groups of metabolically-active rhizosphere microorganisms by stable isotope probing of PLFAs. Soil Biology & Biochemistry **36:**533-537.

44. **Pett-Ridge J, Weber PK.** 2012. NanoSIP: NanoSIMS applications for microbial biology. Methods in molecular biology (Clifton, NJ) **881:**375-408.

45. **Mayali X, Weber PK, Brodie EL, Mabery S, Hoeprich PD, Pett-Ridge J.** 2012. High-throughput isotopic analysis of RNA microarrays to quantify microbial resource use. Isme Journal **6:**1210-1221.

46. **Orphan VJ, House CH, Hinrichs KU, McKeegan KD, DeLong EF.** 2001. Methane-consuming archaea revealed by directly coupled isotopic and phylogenetic analysis. Science **293:**484-487.

47. **Behrens S, Losekann T, Pett-Ridge J, Weber PK, Ng WO, Stevenson BS, Hutcheon ID, Relman DA, Spormann AM.** 2008. Linking microbial phylogeny to metabolic activity at the single-cell level by using enhanced element labeling-catalyzed reporter deposition fluorescence in situ hybridization (EL-FISH) and NanoSIMS. Applied and Environmental Microbiology **74:**3143-3150.

48. **Urbach E, Vergin KL, Giovannoni SJ.** 1999. Immunochemical detection and isolation of DNA from metabolically active bacteria. Applied and Environmental Microbiology **65:**1207-1213.

49. **Goldfarb KC, Karaoz U, Hanson CA, Santee CA, Bradford MA, Treseder KK, Wallenstein MD, Brodie EL.** 2011. Differential growth responses of soil bacterial taxa to carbon substrates of varying chemical recalcitrance. Frontiers in Microbiology **2**.

50. **Hellman M, Berg J, Brandt KK, Hallin S.** 2011. Survey of bromodeoxyuridine uptake among environmental bacteria and variation in uptake rates in a taxonomically diverse set of bacterial isolates. Journal of Microbiological Methods **86:**376-378.

51. **Nannipieri P, Ascher J, Ceccherini MT, Landi L, Pietramellara G, Renella G.** 2003. Microbial diversity and soil functions. European Journal of Soil Science **54:**655-670.

52. **Stotzky G, Norman AG.** 1961. Factors limiting microbial activities in soil. Archiv fur Mikrobiologie **40:**341-369.

53. **Manefield M, Griffiths RI, Bailey MJ, Whiteley AS.** 2006. Stable isotope probing: A critique of its we in linking phylogeny and function. Nucleic Acids and Proteins in Soil **8:**205-216.

54. **Blazewicz SJ, Schwartz E.** 2011. Dynamics of O-18 Incorporation from H (2) (18) O into Soil Microbial DNA. Microbial Ecology **61:**911-916.

55. **Schwartz E.** 2007. Characterization of growing microorganisms in soil by stable isotope probing with H218O. Appl Environ Microbiol **73:**2541-2546.

56. **Nannipieri P, Johnson RL, Paul EA.** 1978. Criteria for measurement of microbial-growth and activity in soil. Soil Biology & Biochemistry **10:**223-229.

57. **McMahon SK, Wallenstein MD, Schimel JP.** 2009. Microbial growth in Arctic tundra soil at-2 degrees C. Environmental Microbiology Reports **1:**162-166.

738 58. **Peterson BJ, Fry B.** 1987. Stable Isotopes in Ecosystem Studies. Annual Review of
739 Ecology and Systematics **18:**293-320.
740 59. **Schimel DS.** 1993. Isotopic Techniques in Plant, Soil and Aquatic Biology: Theory and
741 application of tracers.
742 60. **Mayali X, Weber PK, Pett-Ridge J.** 2013. Taxon-specific C/N relative use efficiency
743 for amino acids in an estuarine community. Fems Microbiology Ecology **83:**402-412.
744
745

Figure Legends

Figure 1. Conceptual model of the quantitative stable isotope probing technique, from sample collection to determining the density of 16S rRNA gene fractions for individual taxa and their corresponding values of atom % stable isotope composition. Note: except for the addition of the stable isotope tracer at the beginning of the incubation, all steps are applied identically to both labeled and unlabeled samples. Artwork by Victor Leshyk.

Figure 2 (A) The ^{18}O composition of *E. coli* DNA as a function of the ^{18}O composition of water in the growth medium. Solid line is the regression ($^{18}O_{DNA}$ = 0.3339 x $^{18}O_{H2O}$ + 0.0004, n=15, $P<0.001$, $R^2=0.976$). (B) The average density of *E. coli* DNA as a function of the ^{18}O composition of the DNA (density = 0.0644 x atom fraction ^{18}O + 1.6946 $R^2 = 0.852$, n=15)

Figure 3. The relative abundance of bacterial 16S rRNA genes, measured through quantitative PCR, as a function of density of DNA. Isotope treatments are shown with filled symbols while natural abundance controls are shown with open symbols. Comparison of soil samples incubated with (A) ^{12}C-glucose and ^{13}C-glucose, (B) ^{16}O-H_2O and ^{18}O-H_2O, and (C) ^{16}O-H_2O plus ^{12}C-glucose and ^{18}O-H_2O plus ^{12}C-glucose. The dotted lines represent the density that separates labeled from non-labeled DNA in traditional SIP. The distribution of densities in each replicate tube yielded an estimate of the average density for that tube, indicated by the horizontal position of the large symbols and error bars at the top of each panel (bars show 90% CIs, with n=3; the vertical position of these symbols does not convey meaning).

Figure 4. Frequency distribution of the 16S rRNA gene as a function of density of DNA for three bacterial taxa without added glucose (left panels) and with added (natural abundance $\delta^{13}C$) glucose (right side panels) for three different taxa: unidentified genera in the families Micrococacceae (A & B) and Pseudonocardiaceae (C & D), and genus *Herpetosiphonales* (E & F). Open symbols and dashed lines show the density distribution for the incubation where all substrates had natural abundance isotope composition, and filled symbols and solid lines show the distribution with ^{18}O-water. Different shapes represent individual replicates within a treatment combination. For each replicate, the area under the curve sums to 1. The distribution of densities for each taxon in each replicate yielded an estimate of the average density for that taxon, indicated by the horizontal position of the large symbols and error bars at the top of each panel (bars show 90% CIs, with n=3; note, the vertical position of the large symbols does not convey meaning).

Figure 5. The taxon-specific shift in average density of DNA (g cm^{-3}, lower horizontal axis) and the corresponding atom fraction excess of ^{18}O or ^{13}C (upper horizontal axis) between incubations with enriched and natural abundance substrates. Changes in DNA density were caused by ^{18}O incorporation from water (A) without or (B) with added natural abundance glucose, or by (C) ^{13}C incorporation from added ^{13}C-labeled glucose. Bars show bootstrapped medians and 90% CIs.

Figure 6. Atom fraction ^{13}C with added ^{13}C-glucose and the shift in atom fraction ^{18}O caused by added ^{12}C-glucose across groups of bacteria. The solid black line represents the expected relationship if organisms derived 100% of their carbon from the added glucose and 33% of their oxygen from ^{18}O water. The difference between the solid line and points falling above it is the indirect effect of added glucose on the utilization of other carbon substrates, reflecting the difference between the total growth stimulation caused by glucose addition and the stimulation based on direct reliance on the added glucose. Points show means with standard errors of the mean (n=3).

Table 1. Definitions of indices, variables, and calculated quantities used in modeling excess atom fraction ^{18}O for each bacterial taxon.

Indices:

i	taxon
j	replicate (or tube) within a treatment
k	fraction (within a replicate)
I	number of taxa
J	number of replicates (within a treatment)
K	number of fractions (within a replicate)

Variables:

f_{jk}	total number of 16S rRNA gene copies per µL (all taxa combined) in fraction k of replicate j (copies μL^{-1})

p_{ijk} proportion of the total number of 16S rRNA gene copies per µL that are taxon *i* in fraction *k* of replicate *j* (unitless)

x_{jk} density of fraction *k* of replicate *j* (g cm^{-3})

Calculated quantities:

y_{ijk} number of 16S rRNA gene copies per µL of taxon *i* in fraction *k* of replicate *j* (copies μL^{-1})

y_{ij} total number of 16S rRNA gene copies per µL of taxon *i* in replicate *j* (copies μL^{-1})

W_{ij} observed weighted average density for taxon *i* in replicate *j* (g cm^{-3})

W_{LABi} mean observed weighted average density for taxon *i* in the labeled treatment (mean across all replicates of the treatment with the heavy isotope) (g cm^{-3})

W_{LIGHTi} mean observed weighted average density for taxon *i* in the unlabeled (i.e., natural abundance) treatment (mean across all replicates in all treatments without heavy isotopes) (g cm^{-3})

G_i guanine + cytosine content of taxon *i* (unitless)

$H_{CARBONi}$ average number of carbon atoms per DNA nucleotide for taxon *i*

M_{LIGHTi} observed molecular weight of the DNA fragment containing the 16S RNA gene for taxon *i* in the unlabeled (i.e., natural abundance) treatment (g mol^{-1})

$M_{HEAVYMAXi}$ theoretical molecular weight of the DNA fragment containing the 16S RNA gene for taxon *i* assuming maximum labeling by the heavy isotope (g mol^{-1})

833 M_{LABi} observed molecular weight of the DNA fragment containing the 16S RNA gene

834 for taxon *i* in the labeled treatment (g mol^{-1})

835 Z_i difference in observed weighted average densities of taxon *i* for the labeled and

836 unlabeled treatments (g cm^{-3})

837 $A_{OXYGENi}$ excess atom fraction of ^{18}O in the labeled versus unlabeled treatment for taxon *i*

838 (unitless)

839 $A_{CARBONi}$ excess atom fraction of ^{13}C in the labeled versus unlabeled treatment for taxon *i*

840 (unitless)

841

842

Table 2. Density (g cm^{-3}) of DNA for taxa exhibiting or not exhibiting tracer assimilation in the three tracer experiments. Values are means and standard deviations.

	Density (g cm^{-3})	
Tracer	assimilating	not assimilating
^{18}O-H_2O	1.6905 ± 0.0031	1.6912 ± 0.0033
^{18}O-H_2O with glucose	1.6896 ± 0.0033	1.6894 ± 0.0045
^{13}C-glucose	1.6890 ± 0.0030	1.6900 ± 0.0036

843

844 Figure 1.

845

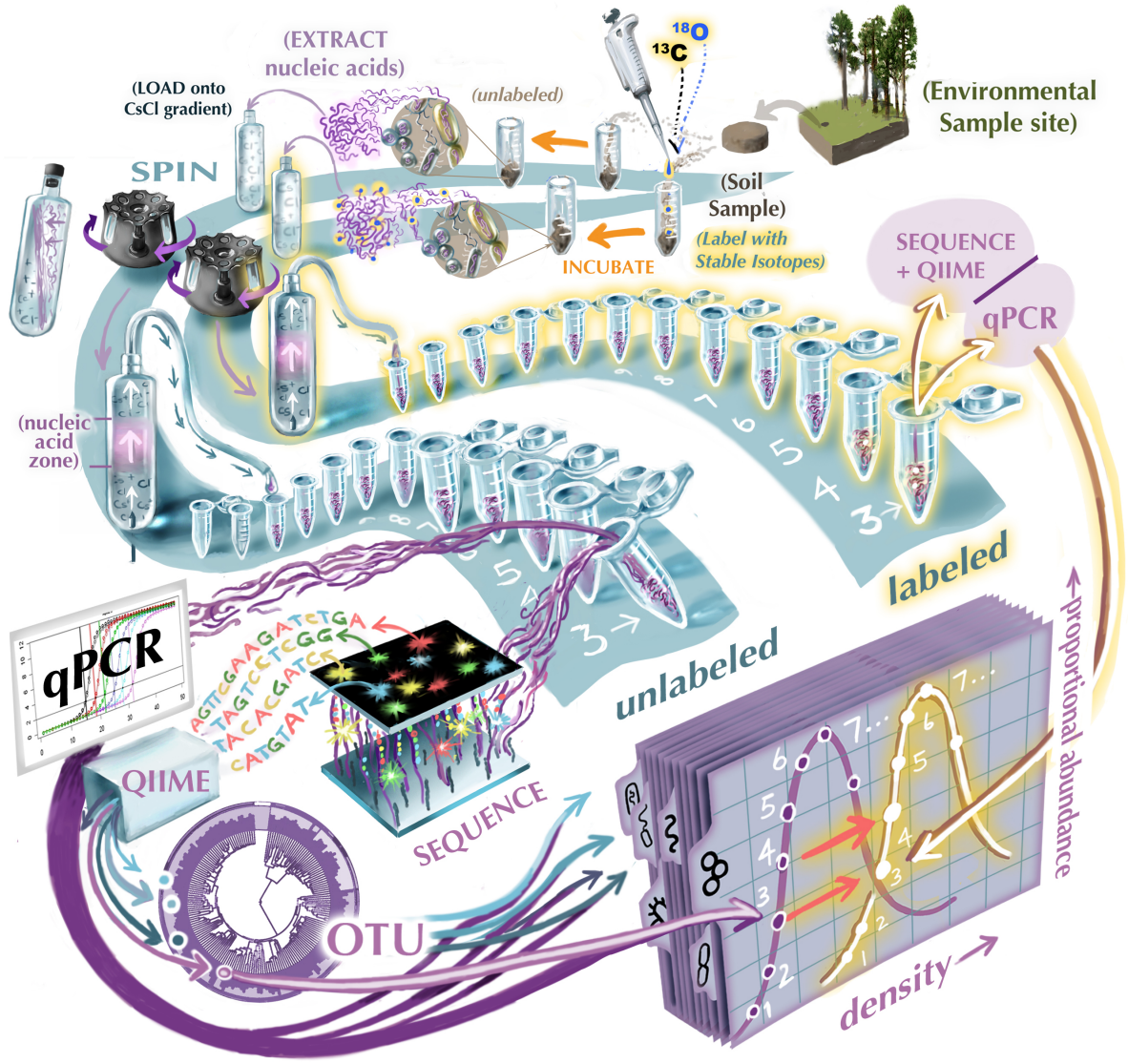

846

847
848
849
850
851
852
853
854
855

856 Figure 2
857

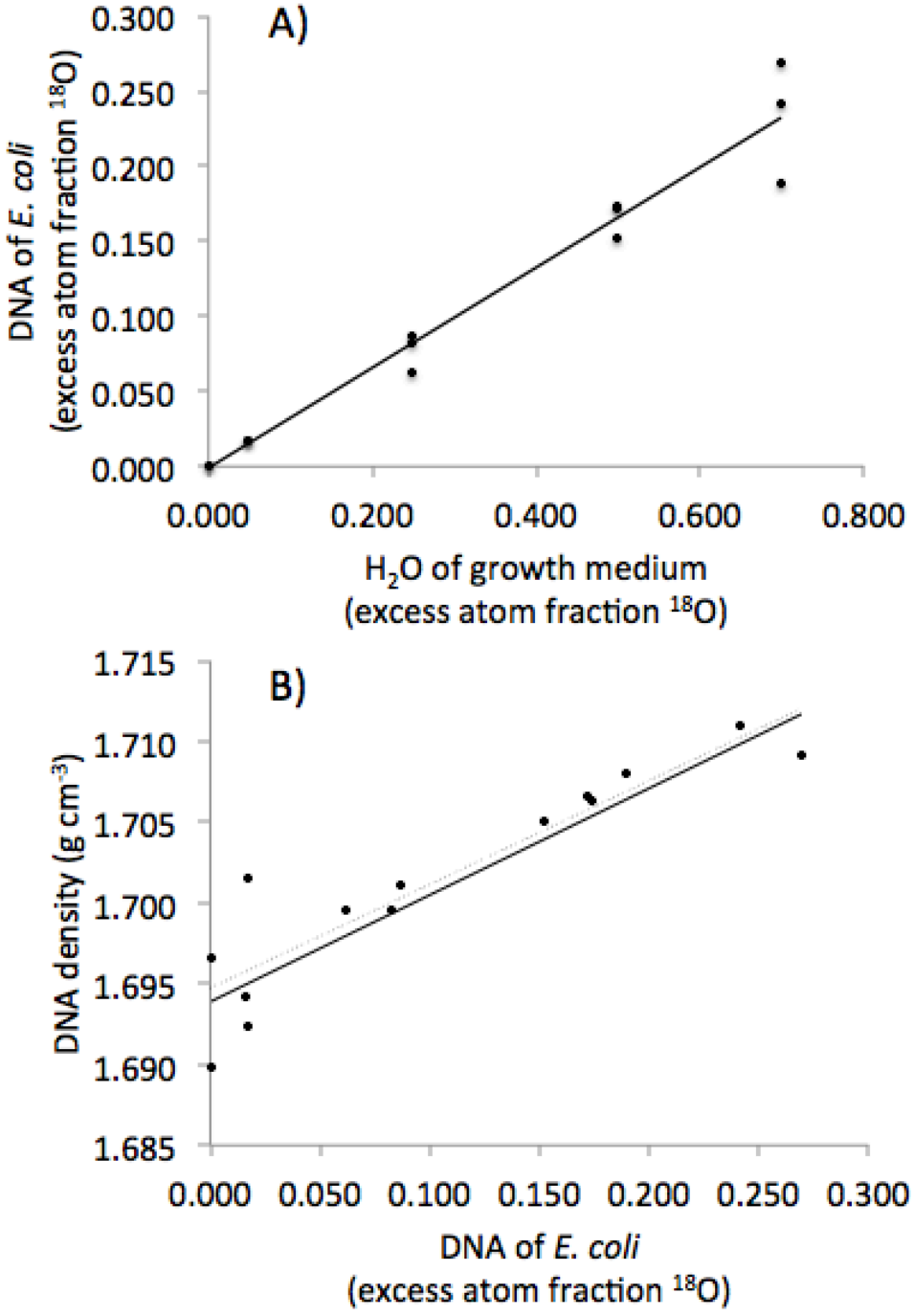

858
859
860
861

Figure 3.

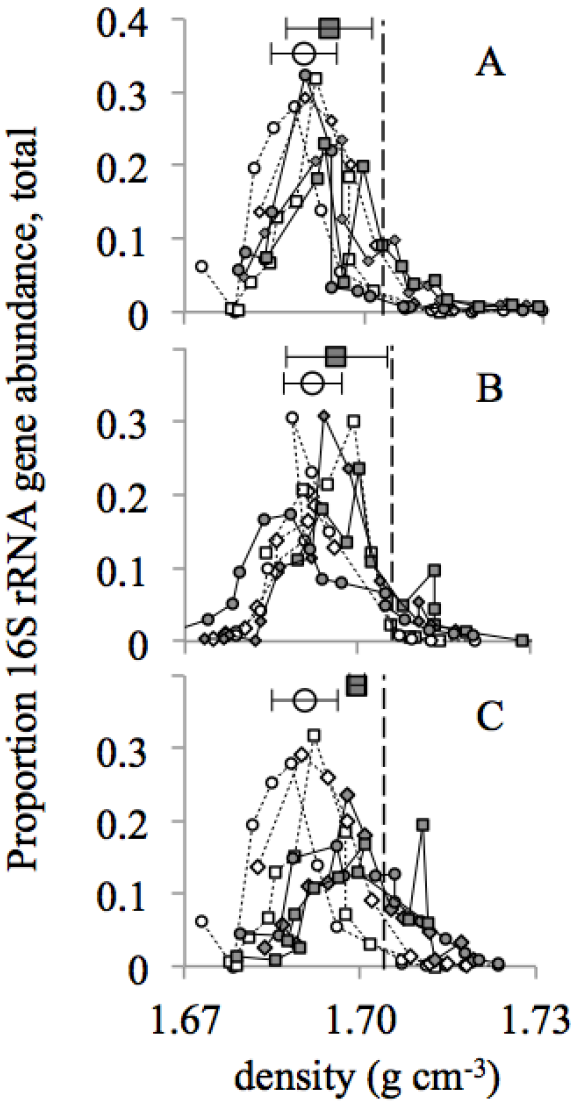

876 Figure 4
877
878

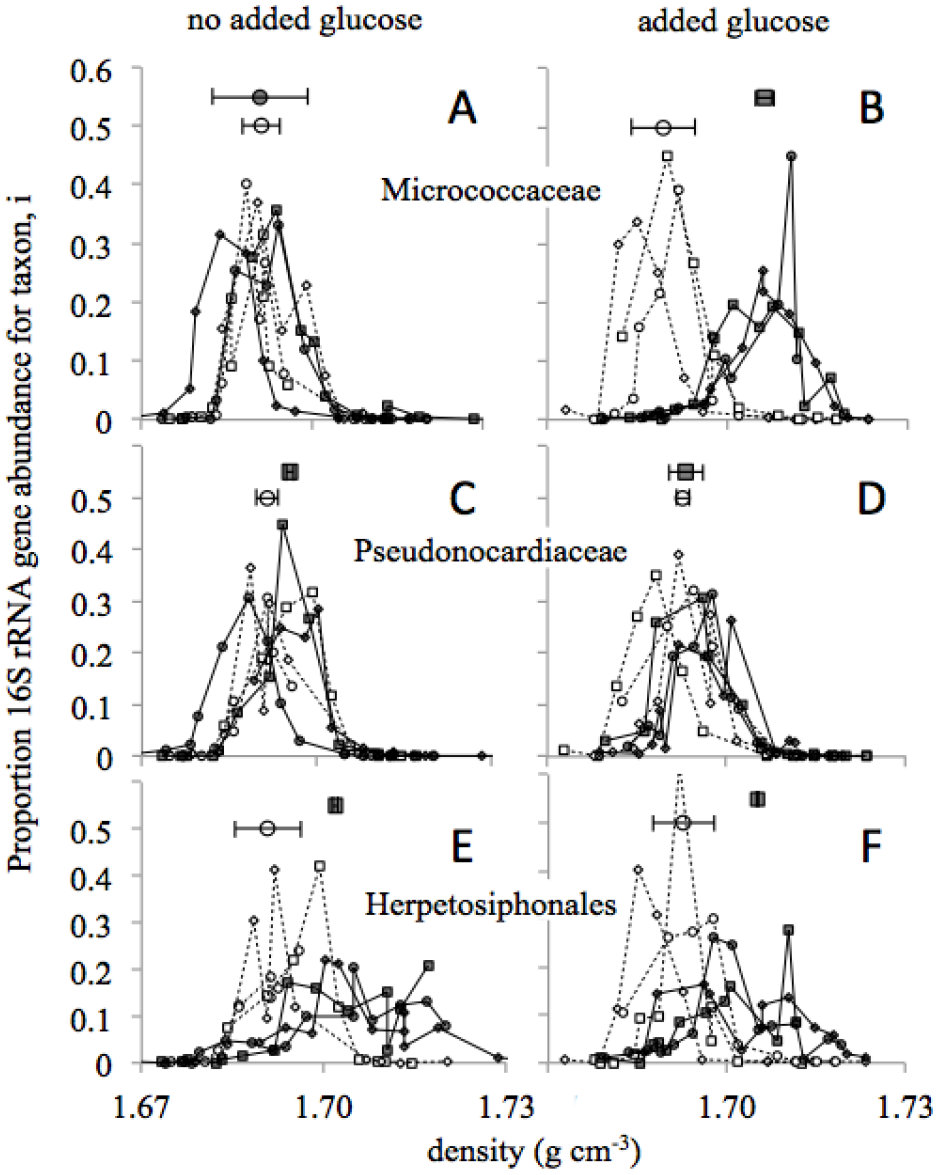

879 Figure 5.
880

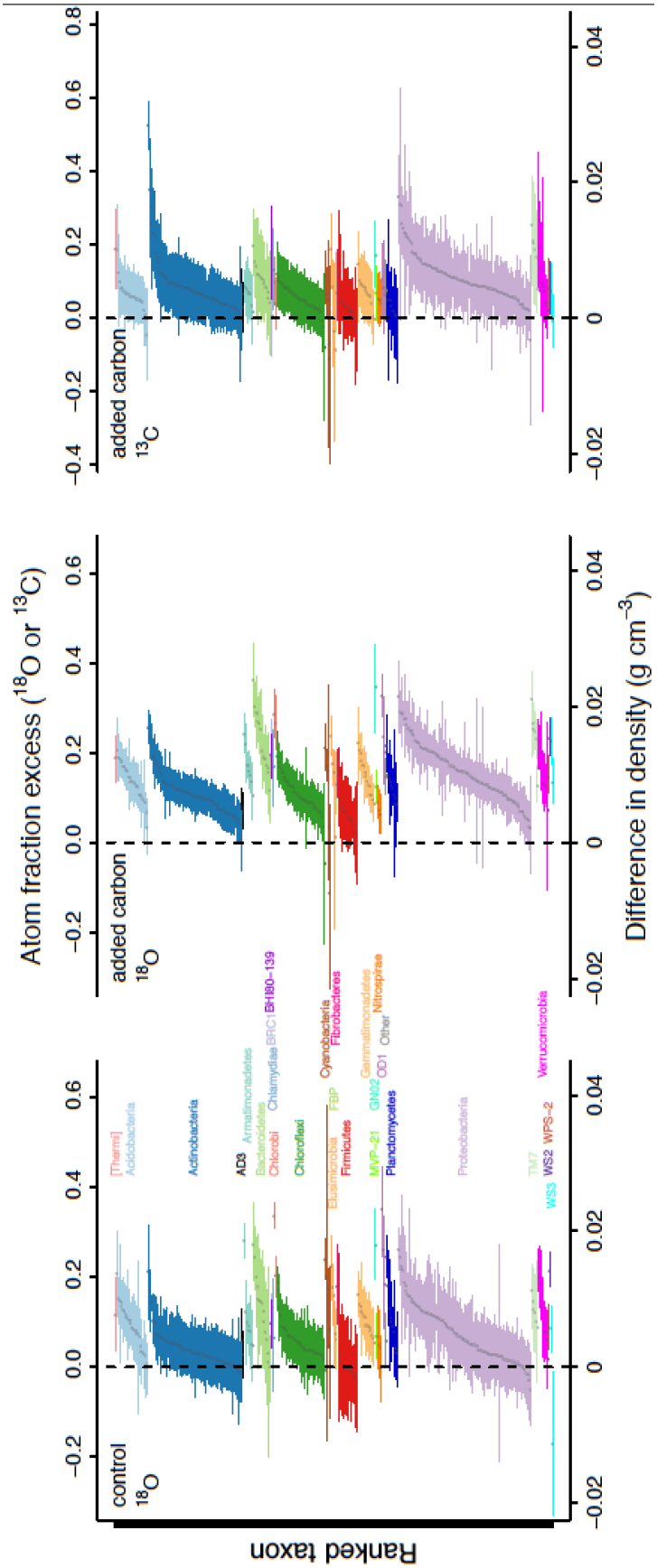

881 Figure 6.
882
883